Short-Period Modulations in Aerosol Optical Depths over the Central Himalayas: Role of Mesoscale Processes

U. C. DUMKA
Aryabhatta Research Institute of Observational Sciences, Manora Peak, Nainital, India

K. KRISHNA MOORTHY
Space Physics Laboratory, Vikram Sarabhai Space Center, Thiruvananthapuram, India

S. K. SATHEESH
Center for Atmospheric and Oceanic Sciences, Indian Institute of Science, Bangalore, India

RAM SAGAR AND P. PANT
Aryabhatta Research Institute of Observational Sciences, Manora Peak, Nainital, India

(Manuscript received 7 November 2006, in final form 7 September 2007)

ABSTRACT

Multiyear measurements of spectral aerosol optical depths (AODs) were made at Manora Peak in the central Himalaya Range (29°22′N, 79°27′E, ~1950 m above mean sea level), using a 10-channel multiwavelength solar radiometer for 605 days during January 2002–December 2004. The AODs at 0.5 μm were very low ($\leq$0.1) in winter and increased steeply to reach high values (~0.5) in summer. It was observed that monthly mean AODs vary significantly (by more than a factor of 6) from January to June. Strong short-period fluctuations (within a daytime) were observed in the AODs. Further investigations of this aspect have revealed that boundary layer dynamics plays a key role in transporting aerosols from the polluted valley region to higher altitudes, causing large contrast in AODs between forenoon and afternoon. The seasonal variations in AODs, while examined in conjunction with synoptic-scale wind fields, have revealed that the transport of dust aerosols from arid regions to the valley regions adjacent to the observational site and their subsequent transport upward by boundary layer dynamics are responsible for the summer increases.

1. Introduction

Long-term observations of aerosol characteristics are important in characterizing their spatiotemporal heterogeneities as well as in evolving climatological models for radiation budget studies. Numerous measurements and impact assessments have been reported from the Indian region in recent years (Satheesh and Ramanathan 2000; Ramanathan et al. 2001; Babu et al. 2002; Tripathi et al. 2005). However, most of these studies have focused on either the urban–semiurban landmasses or the oceans adjacent to the densely populated coastal belt. Investigations from remote, sparsely inhabited regions have the benefit of providing a sort of background against which the urban impacts can be compared. From this perspective, observations from high-altitude stations have significance as the aerosols in this region provide a "far-field picture," being quite a distance away from potential sources and are more representative of free-troposphere conditions. Recent observations have revealed pockets of high aerosol loading–optical depth in the north Indian regions around the Ganga basin, particularly during the winter season when the prevailing meteorological conditions are favorable (Di Girolamo et al. 2004; Tripathi et al. 2005; Jethva et al. 2005). The observations from high-altitude stations are important, as they are essential in assessing the impacts of human activities on free-tropospheric aerosols and also in the modeling boundary layer to free-troposphere mass exchanges. Furthermore, most of the aerosol sources are located close to the earth's surface and observations from high-altitude locations provide an opportunity to investigate their

Corresponding author address: S. K. Satheesh, Center for Atmospheric and Oceanic Sciences, Indian Institute of Science, Bangalore 560012, India.
E-mail: satheesh@caos.iisc.ernet.in

DOI: 10.1175/2007JAMC1638.1

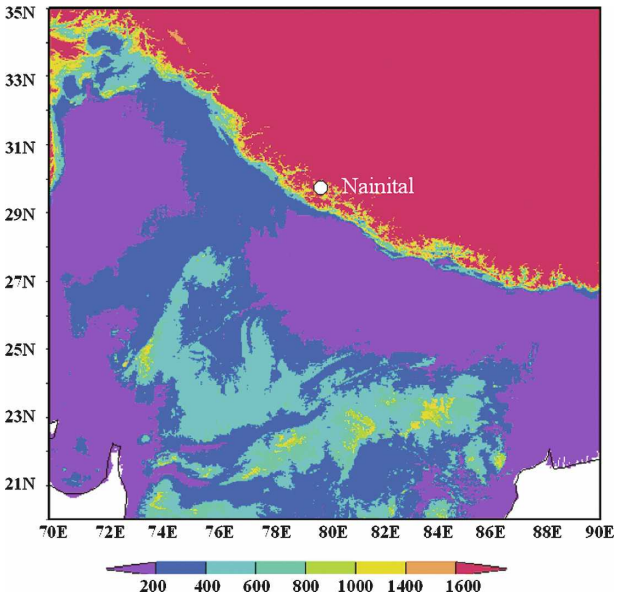

FIG. 1. The geographical location of Manora Peak over the Indian subcontinent. Color code represents topographical features (m).

features from locations where most of the source fluctuations are smaller. The spectral aerosol optical depth (AOD) is a key parameter in order to build up a comprehensive picture of aerosols and their potential environmental impacts (Moorthy et al. 1999; Satheesh et al. 2002). Extensive measurements of spectral AODs from a high-altitude Indian station (Manora Peak in the Shivalik Hills of the central Himalaya Range) was initiated in January 2002, using a multiwavelength solar radiometer (MWR) under the Indian Space Research Organization's Geosphere and Biosphere Program (ISRO-GBP) (Sagar et al. 2004). In this paper, we have used an extensive database of aerosol spectral optical depths spread over 3 yr (January 2002–December 2004) to study aerosols at high altitudes and to examine the possible role of synoptic- and mesoscale systems on seasonal and short-period variations in aerosol properties. The results and its implications are discussed.

2. Details of location and measurements

The experimental site, Manora Peak (29°22′N, 79°27′E, ~1950 m above mean sea level) is located to the south of the hill station, Nainital (see Fig. 1), which has a total population of around 70 000. The site lies in the Manora Peak, Nainital in the central Himalayas. The color code in Fig. 1 indicates the topographical features of the region surrounding Nainital. The foothill stations are located to the southwest of the site at an aerial distance of around 10 km and about 300 m above mean sea level. Farther to the west lies densely populated regions including the Indian capital (New Delhi) and the southern region includes heavily the populated Gangetic plains. To the northeast of the Manora Peak is the hilly terrain of the central Himalayan ranges (>2.0 km MSL), which have essentially no anthropogenic activities and are rather pristine. To the south and southwest are densely populated valley regions (at a mean elevation of ~300 m).

TABLE 1. Number of days of observations.

Month	2002	2003	2004
Jan	12	27	22
Feb	11	16	23
Mar	21	24	30
Apr	21	27	15
May	10	29	29
June	7	10	15
July	—	—	6
Aug	—	—	—
Sep	5	4	15
Oct	25	29	16
Nov	27	26	27
Dec	24	26	26
Total	163	218	224

Regular and continuous measurements of spectral AODs have been carried out since January 2002 from Manora Peak, Nainital, using a multiwavelength solar radiometer described in detail elsewhere (Moorthy et al. 1999; Sagar et al. 2004). The MWR instrument has a field of view of 2° and measures AODs at 10 narrow-wavelength bands centered at 0.38, 0.40, 0.45, 0.50, 0.60, 0.65, 0.75, 0.85, 0.935 and 1.025 μm (with full-width half-maximum bandwidths between 4 and 6 nm). The instrumental details, methods of analysis, and error budget are described in Moorthy et al. (1999) and Sagar et al. (2004). The overall error in the estimation of AOD values is in the range ~0.02–0.04 at different wavelengths (Shaw 1976). A monthly distribution of the datasets (from January 2002 to December 2004) is presented in Table 1. In all, 605 days of observations were made during the period under investigation. The monthly database set is generally strong for most of the period except during July–September, when the extensively cloudy conditions make it difficult to make observations.

3. General meteorological conditions

Regular measurements of the surface meteorological parameters such as wind direction (θ, °), wind speed (U, m s^{-1}), relative humidity (RH, %), temperature (T, °C), and total rainfall (RF, cm) are recorded at the site using a set of weather instruments. The monthly

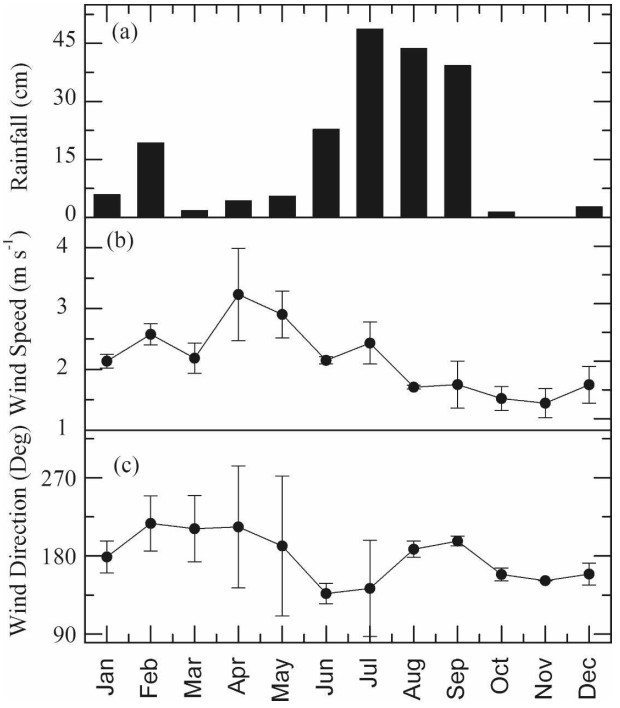

FIG. 2. Variations of (top) monthly total rainfall, (middle) monthly mean wind speed, and (bottom) wind direction measured clockwise from the north. The vertical bars through the solid points are the standard errors.

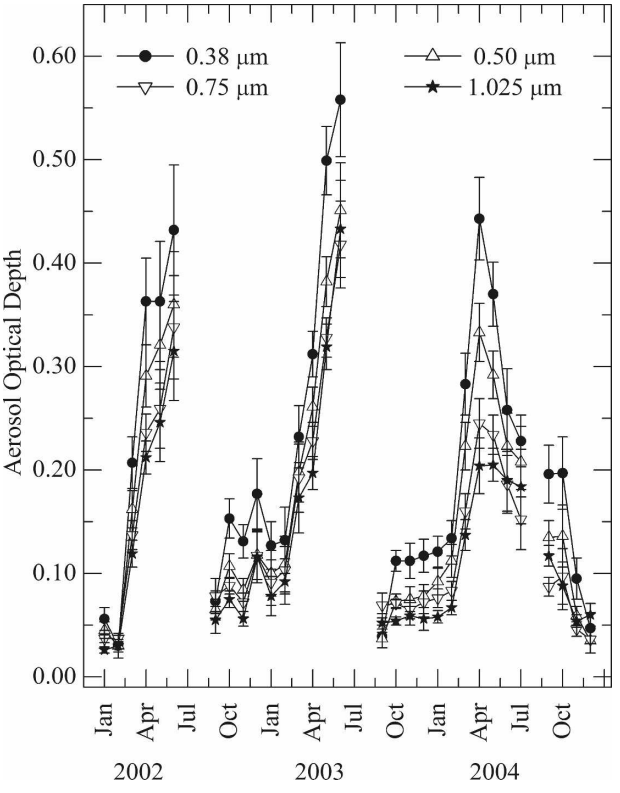

FIG. 3. Monthly variations of AOD at Manora Peak, Nainital for the period 2002–04 at four representative wavelengths (0.38, 0.50, 0.75, and 1.025 μm), two in the visible region and two in the near IR.

mean values of RF, U, and θ during the period under study are shown in Fig. 2. Winds are generally westerly and northwesterly during November–May, shifting to westerly–southwesterly during June–September. Generally, the monthly mean wind speeds are low (<5 m s^{-1}) for most of the year. The rainfall is significant in February (caused by western disturbances) and during June–September (the Indian summer monsoon season), which account for about 68% of the annual rainfall. The western disturbances (WDs) usually originate usually over the Mediterranean Sea–Black Sea areas or the west Atlantic, as extratropical frontal systems, but their frontal properties are lost while moving eastward toward India across Afghanistan–Pakistan. However, even then, an intense WD is capable of producing widespread heavy snowfall–rainfall over the Himalayan region and rains over the northern plains of India. The RH during daytime is generally <50% during November–April and thereafter increases steadily and reaches a peak value of ~75%–85% during June–September (the monsoon period).

4. Results and discussions

In the following, we examine the temporal and spectral features in AOD and possible linkages of these to the changes in prevailing meteorological conditions.

a. Temporal variation of AODs

Monthly variations of AOD at Manora Peak, Nainital, are presented in Fig. 3 at four representative wavelengths (0.38, 0.50, 0.75, and 1.025 μm; two in the visible region and two in the near IR). The individual points are the monthly mean AOD, obtained as the arithmetic mean of all of the AOD values for that month, and the vertical bars through the points are the standard error ($1/\sqrt{N}$ times the ensemble standard deviations, N being the number of individual AOD values in the ensemble) of the mean value. The monthly mean AOD values for different years separately are provided in Table 2. The following results were found:

1) Low AOD values (<0.1) are encountered frequently during November–February. Higher values occurred more frequently in March–June. AOD is at aminimum during January and increases in summer (April–June) reaching values as high as ~0.5.
2) Variations in AOD within a month are generally higher during April–June while they are quite small during November–February.
3) At all wavelengths, monthly mean variations of AODs showed nearly similar patterns for all years.

TABLE 2. Monthly mean AOD at 0.50 μm.

Month	2002	2003	2004
Jan	0.04 ± 0.01	0.10 ± 0.02	0.09 ± 0.01
Feb	0.03 ± 0.01	0.11 ± 0.03	0.11 ± 0.02
Mar	0.16 ± 0.02	0.20 ± 0.03	0.22 ± 0.03
Apr	0.29 ± 0.03	0.26 ± 0.02	0.33 ± 0.03
May	0.32 ± 0.04	0.38 ± 0.02	0.29 ± 0.02
Jun	0.36 ± 0.05	0.45 ± 0.05	0.22 ± 0.04
Jul	—	—	0.21 ± 0.03
Aug	—	—	—
Sep	0.06 ± 0.01	0.04 ± 0.01	0.14 ± 0.02
Oct	0.11 ± 0.01	0.07 ± 0.01	0.14 ± 0.03
Nov	0.08 ± 0.01	0.08 ± 0.01	0.06 ± 0.01
Dec	0.12 ± 0.02	0.08 ± 0.01	0.03 ± 0.01

However, during 2004 there was a discrepancy in this trend during May and June in comparison to 2002 and 2003. This could be due to the fact that a good amount of intermittent rain occurred during these months in 2004, consequently decreasing the value of the AODs.

To study the seasonal variation in AOD values, the AOD data are grouped into four seasons, namely winter (November–February), summer (premonsoon) (March–June), monsoon (July–August), and postmonsoon (September–October). The mean AOD values at $\lambda = 0.5$ μm for each season are plotted in Fig. 4. The seasonal variations in AODs indicate high AOD values

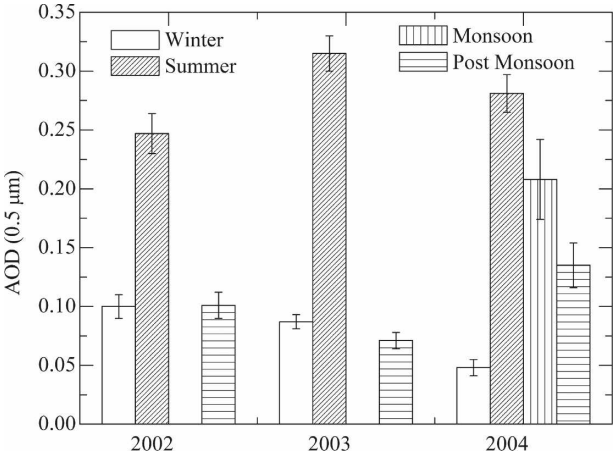

FIG. 4. Mean AODs at 0.5 μm for the winter (November–February), summer (premonsoon) (March–June), monsoon (July–August) and postmonsoon (September–October) seasons.

in summer and low values in winter. The AOD values are slightly higher in the monsoon and postmonsoon seasons of 2004 due to the scant rainfall during the period, while during 2002 and 2003 there was an absence of AOD data.

The frequency distributions of AODs during winter (top panel) and summer (bottom panel) seasons at four representative wavelengths (0.38, 0.50, 0.75, and 1.025 μm) are shown in Fig. 5. It was observed that during the summer, about 90% of the values of AODs

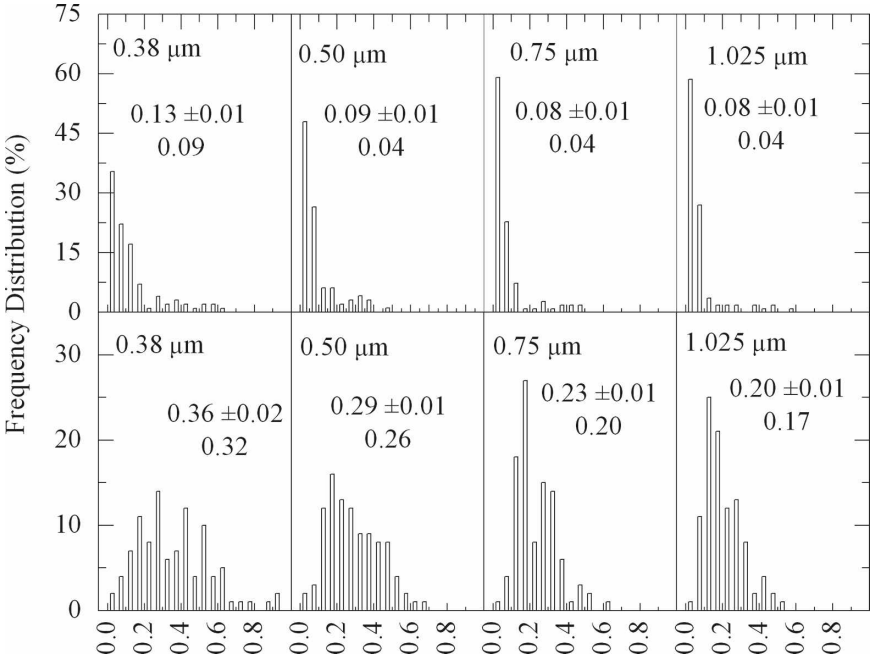

FIG. 5. The frequency distributions of AODs during (top) winter and (bottom) summer seasons at four representative wavelengths (0.38, 0.50, 0.75, and 1.025 μm). Shown in each panel are the mean plus/minus the standard deviation and, below that, the median.

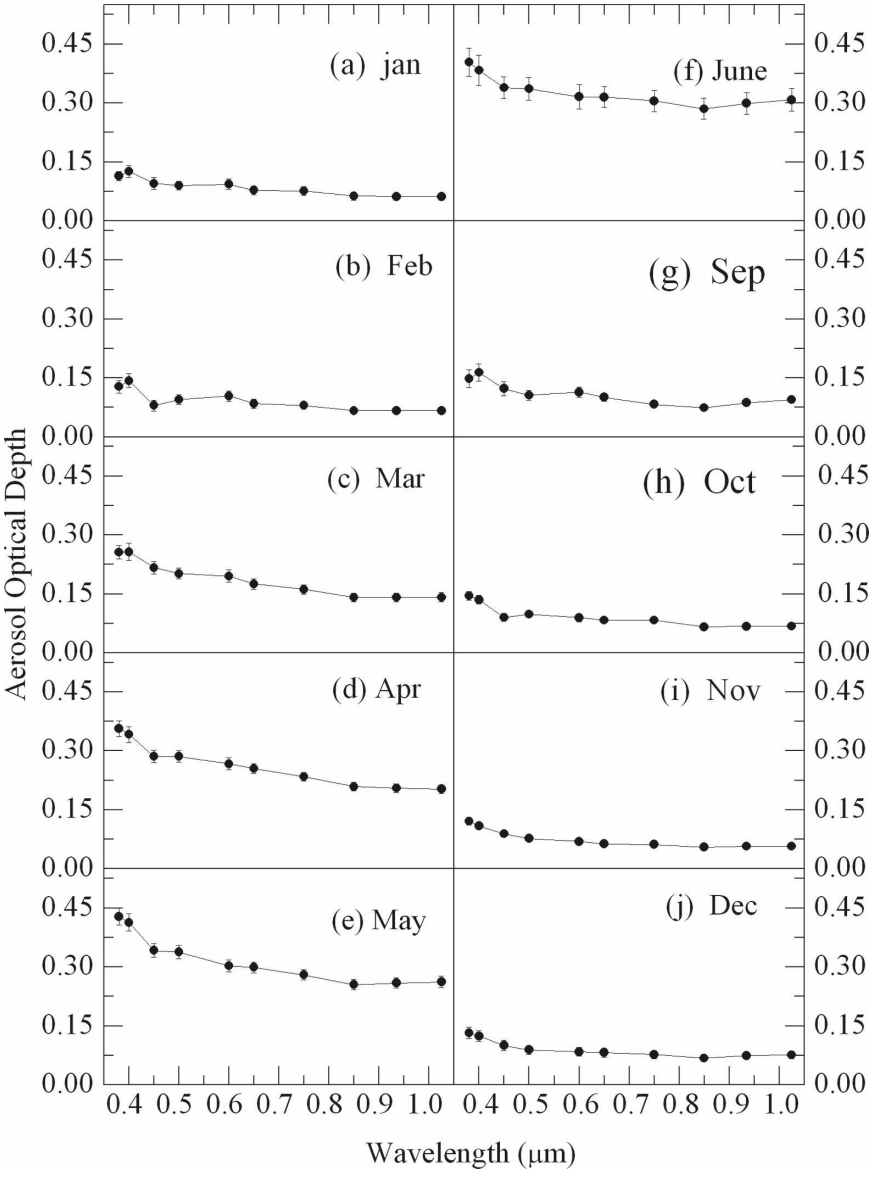

FIG. 6. Variations of monthly mean AODs as a function of wavelength.

fall in the range 0.05–0.5, and in winter 90% of the AODs values fall in the range 0.05–0.2.

b. Spectral variation of AODs

The spectral variation of AODs is important, as it is indicative of the changes in the aerosol size characteristics.

In Fig. 6, the variations of the monthly mean aerosol optical depths are shown as a function of wavelength (λ). In general, AODs show a decreasing trend as λ increases. The spectral variations become less steep during the months of April–June due to the relative increases in the AODs in near-infrared (NIR) wavelengths. The spectral variations of the AODs become steeper during winter months.

Spectral variation of aerosol optical depth ($\tau_{p,\lambda}$) can be expressed following the inverse power-law representation of Ångström (1964) as

$$\tau_{p,\lambda} = \beta\lambda^{-\alpha}, \tag{1}$$

where α is the wavelength exponent, β is the turbidity parameter, and λ is the wavelength (μm). The value of α depends on the ratio of the concentration of large to small particles and β represents the total aerosol loading in the atmosphere (Shaw et al. 1973). Higher values of α thus indicate an aerosol size spectrum with a rela-

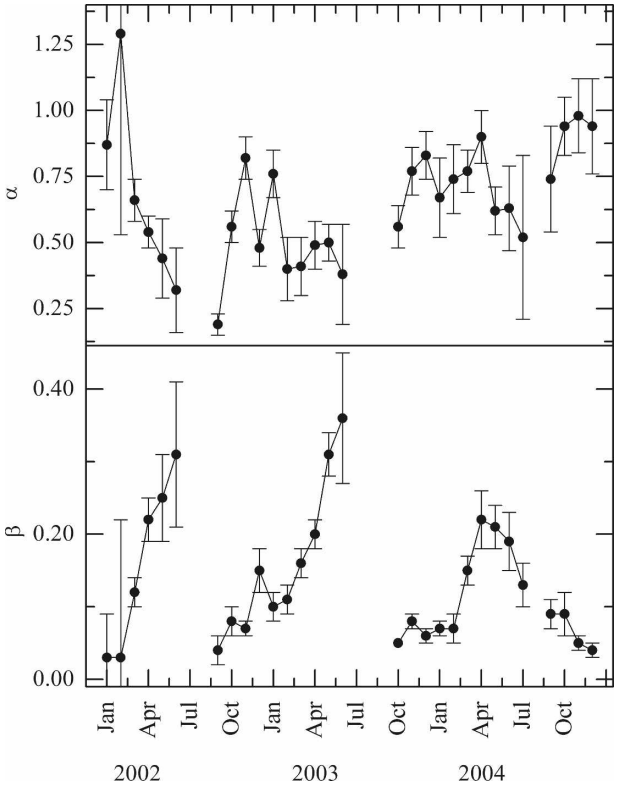

FIG. 7. The monthly mean values of (top) α and (bottom) β for the period 2002–04. The solid points are the respective monthly mean values, and the vertical bars through the solid points are the standard errors.

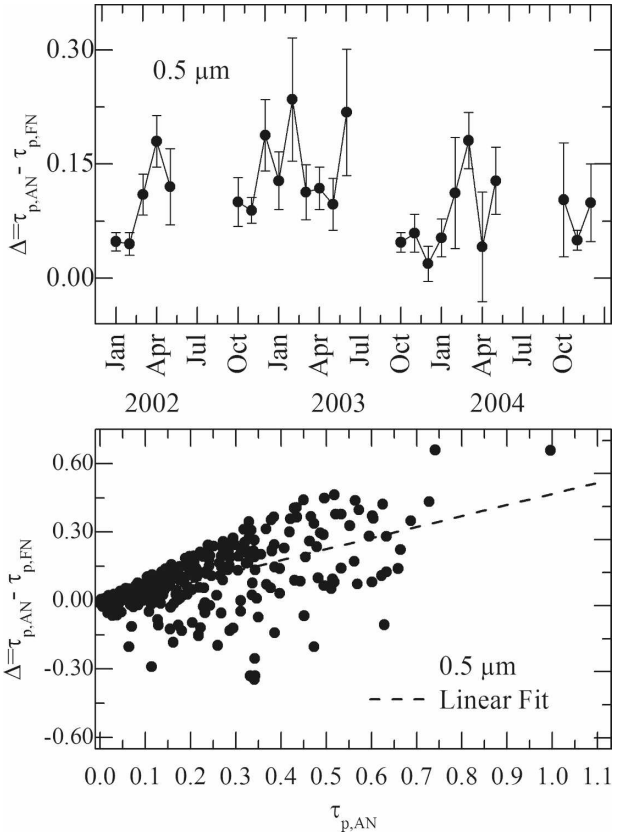

FIG. 8. (top) The AOD difference $\Delta = (\tau_{p,\mathrm{AN}} - \tau_{p,\mathrm{FN}})$ averaged separately for each month for the period 2002–04. (bottom) The scatterplot between Δ and afternoon optical depth ($\tau_{p,\mathrm{AN}}$).

tive dominance of smaller aerosols. The values of α and β are obtained by least squares fitting of $\tau_{p,\lambda}$ versus λ on a log–log scale. The monthly mean values of α and β are plotted in Figs. 7a and 7b. It was observed that the average value of α decreases systematically from January to March (during 2002 and 2003) and remains at that level during summer, indicating a systematic increase in the relative abundance of large aerosol in the size spectrum. This could be attributed partly to changes in the synoptic conditions, which are conducive for the advection of dust aerosols from the west Asian and western Indian arid regions by favorable winds. The value of α was high during winter months and minimum during summer. On the other hand, β was found to be maximum during summer and minimum during the winter season. These results indicate that there is a relative dominance of submicron particles during the winter season and a dominance of coarse particles during the summer season.

c. *Role of boundary layer dynamics on the short-period fluctuations*

Examination of instantaneous AODs has revealed significant variations within the daytime. The variations in the AODs at very short-term scales (within a day) are therefore investigated. Out of 605 observation days (during 2002–2004), there are 316 days where both forenoon (FN) and afternoon (AN) AOD observations are available. The difference between FN and AN AODs, $\Delta = (\tau_{p,\mathrm{AN}} - \tau_{p,\mathrm{FN}})$, is estimated on all of these days. Considering the uncertainties in the AOD estimations, a difference in the AODs of less than 0.04 (i.e., $|\Delta| < 0.04$) is considered to be insignificant. The number of data points in the range $\Delta < -0.04$, $-0.04 < \Delta < +0.04$, and $\Delta \geq 0.04$ are 35, 106, and 175, respectively. Examining from the above perspective, it was found that for nearly 75% of the case covered $\Delta > +0.04$, indicating that on most of the days, the AODs are higher in the AN than in the FN. The deviations, $\Delta = (\tau_{p,\mathrm{AN}} - \tau_{p,\mathrm{FN}})$, of FN and AN AODs are averaged separately for each month and the resulting monthly mean variations are shown in Fig. 8. The figure indicates that generally high AODs persist during the AN relative to the FN, especially during summer. The scatterplot between Δ and the afternoon optical depth ($\tau_{p,\mathrm{FN}}$) is also shown in Fig. 8 (bottom panel).

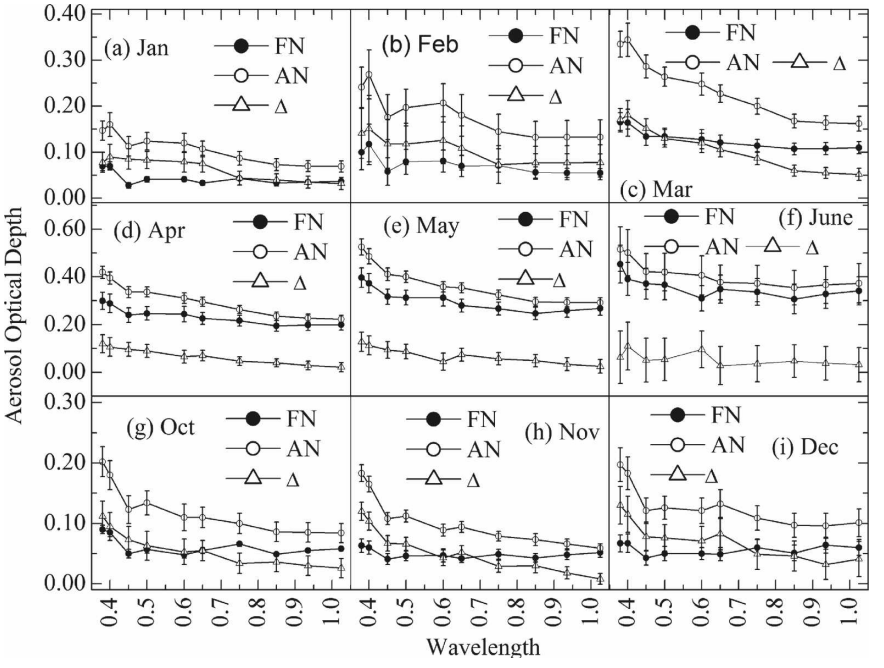

FIG. 9. AODs averaged separately for FN and AN, and their difference Δ as a function of wavelength (μm).

The spectral AODs averaged separately for FN and AN, and their difference (Δ), are shown in Fig. 9. Figures 8 and 9 reveals that the FN to AN changes are significant over the entire MWR wavelength range during March–May. However, the difference is larger at short-wavelength range ($\lambda \leq 0.65$ μm). Figure 10 represents the monthly mean variations of α and β for the FN and AN datasets. It is observed that during the AN period α is high compared to the FN value. The higher value of α during the AN period implies the relative dominance of fine–submicrometer aerosol particles.

The temporal changes in AODs and their λ dependence appear to have been strongly influenced by the dynamics of the boundary layer and its variation over the year associated with the changes in solar heating. During nighttime, the shallow nocturnal boundary layer acts as a capping inversion (Stull 1989), confining the emissions from these regions well below the mountain peak. After sunrise, the heating of the land surface results in setting up of convective motions, which gradually raise the inversion to higher altitudes (Kovalev and Eichinger 2004), leading to increased vertical mixing that brings up the air with high aerosol concentrations to higher levels. This would result in an increase in the concentration of anthropogenic aerosols at Manora Peak, as is observed in the present study.

We have also examined the role of the evolving boundary layer in transporting aerosols from the polluted valley region to Manora Peak. To estimate the

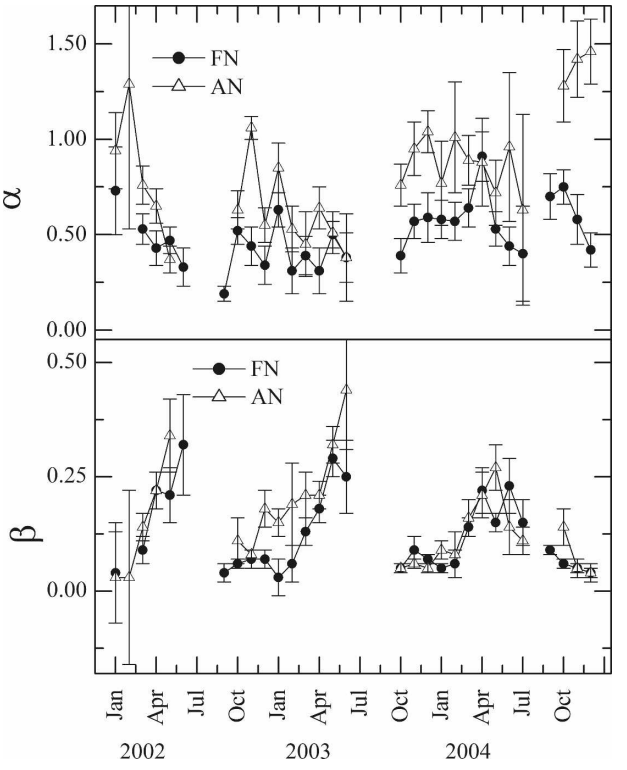

FIG. 10. The monthly mean variations of (top) α and (bottom) β for the period 2002–04 for FN and AN datasets.

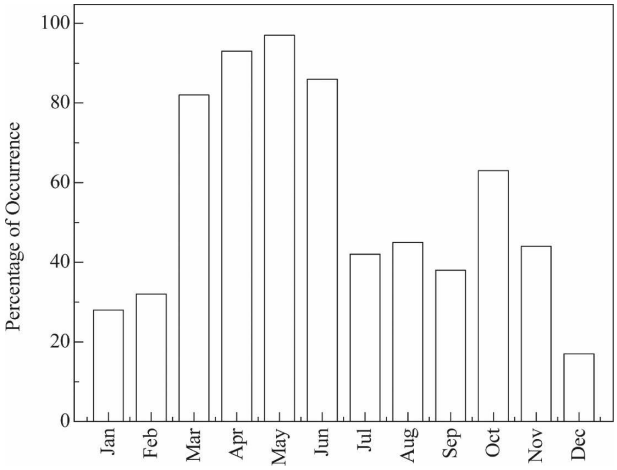

FIG. 11. The percentage of occurrence of mixed layer height exceeding the altitude of Manora Peak (our observation site) during each month for 2003.

mixed layer height, we used radiosonde data (from the nearest India meteorological department, New Delhi). The measured temperature (T) and pressure (P) are used to compute the potential temperature, T_P (Stull 1989):

$$T_P = T\left(\frac{1000}{P}\right)^{0.286}, \tag{2}$$

where P is in hectopascals and T is in kelvin. The altitude profiles of T_P are used to infer the atmospheric boundary layer (ABL) characteristics. During the afternoon, the potential temperature profiles revealed a well-developed ABL. It consists of a surface layer (SL) close to the ground where T_P decreases sharply with altitude, representing a superadiabatic regime. Above the SL, T_P becomes nearly steady with altitude (due to turbulent mixing), representing an adiabatic lapse rate. This region of nearly constant T_P is the well-mixed layer (ML), the base of which is at the top of the SL. In Fig. 11, we show the percentage of occurrence of the mixed layer height exceeding the altitude of Manora Peak (our observation site) during each month. When the mixed-layer height exceeds the altitude of Manora Peak, then aerosols from the polluted valley below reach the observation site. It was observed that during March–June and October, the percentage of occurrence exceeded more than 50%. Further, AODs during the afternoon showed a positive correlation during summer (with a correlation coefficient r of +0.49), with the maximum temperature ($T_{\max}$) observed during the daytime (see Fig. 12). Even though this correlation is not very high, it is significant ($P < 0.001$) for the 46 pairs of observations in Fig. 12. The significant scatter is

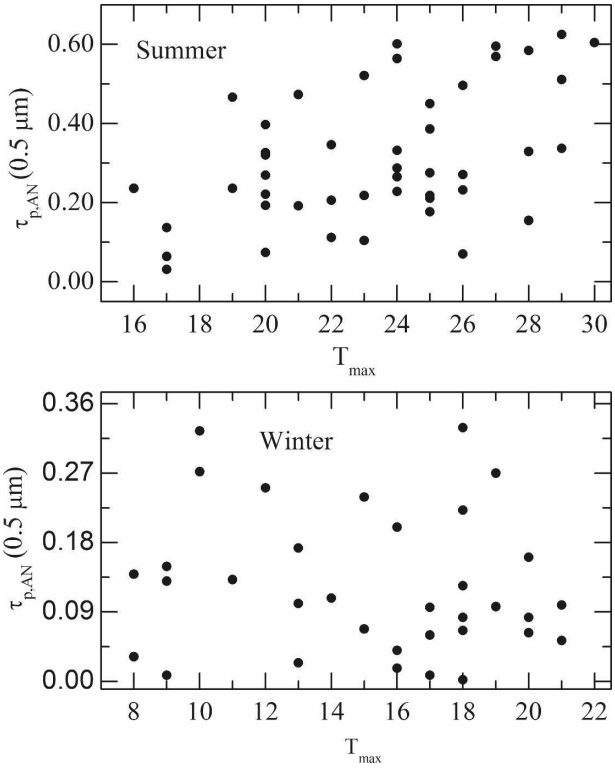

FIG. 12. The scatterplot between AODs during the afternoon and maximum temperature ($T_{\max}$) observed during daytime for (top) summer and (bottom) winter at 5 μm.

attributed to the usage of $T_{\max}$ as a proxy for the strength of convection, which would in turn determine the depth of the ABL. The deeper the ABL, the more efficient will be the lifting of the pollutants from the valley to the peak and the larger will be the increase in the AOD in the afternoon. On the other hand, AODs during the forenoon showed negative correlation (with a correlation coefficient r of −0.13) with $T_{\max}$. The investigations reported above indicate the significant role of boundary layer dynamics in transporting aerosols from the polluted valley to the pristine atmosphere at higher levels.

Similar types of studies have been reported by Bhugwant et al. (2001) in the case of aerosol black carbon. Bhugwant et al. (2000, 2001) showed that the high BC values during the AN period at high-altitude sites can be attributed to the vertical transport of aerosols from the nearby polluted urban and valley regions, which were initially confined to lower heights during the night and early morning hours due to the low-level inversions, but are released to greater heights (~2 km) as the boundary layer evolves. At night, most of the aerosol concentrations are trapped by the low-level capped inversions, and as the land gets heated up during the day,

the increased convective activity leads to a breaking of the capped inversion causing the mixing of aerosols and pollutants vertically and horizontally, thereby leading to increased AODs in the AN period. Aerosols over the Indian subcontinent may have implications for cloud microphysical properties and the radiation budget.

5. Conclusions

Multiyear measurements of spectral aerosol optical depths (AODs) made at Manora Peak in the central Himalayas have revealed the following.

1) The AODs at 0.5 μm were very low ($\leq$0.1) in winter and increased rather steeply to reach high values ($\sim$0.5) in summer.
2) The monthly mean AODs vary significantly (by more than a factor of 6) from January to June.
3) Strong short-period fluctuations (within a daytime) were observed in AODs.
4) The boundary layer dynamics was found to play a key role in transporting aerosols from the polluted valley region to higher altitudes, causing a large contrast in AODs between forenoon and afternoon.
5) The seasonal variation in AODs while examined in conjunction with synoptic-scale wind fields has revealed that the transport of dust aerosols from arid regions to the valley regions adjacent to the observational site and their subsequent transport upward by boundary layer dynamics are responsible for the summer increases.

Acknowledgments. This study is funded under the ISRO-Geosphere Biosphere Program of the Department of Space, government of India. The authors thank the technical staff of the ARIES, Manora Peak, Nainital, for providing valuable help during the observations. The authors thank Brijesh Kumar, Manoj Kumar Srivastava, Auromeet Saha, and P. Hegde for fruitful discussions on certain issues.

REFERENCES

Ångström, A., 1964: Techniques of determining the turbidity of the atmosphere. *Tellus,* **13,** 214–223.

Babu, S. S., S. K. Satheesh, and K. Krishna Moorthy, 2002: Aerosol radiative forcing due to enhanced black carbon at an urban site in India. *Geophys. Res. Lett.,* **29,** 1880, doi:10.1029/2002GL015179.

Bhugwant, C., H. Cachier, M. Bessafi, and J. Leveau, 2000: Impact of traffic on black carbon aerosol concentration at la Reunion Island (southern Indian Ocean). *Atmos. Environ.,* **34,** 3463–3473.

——, M. Bessafi, E. Riviere, and J. Leveau, 2001: Diurnal and seasonal variation of carbonaceous aerosols at a remote MBL site of La Reunion Island. *Atmos. Res.,* **57,** 105–121.

Di Girolamo, D. L., and Coauthors, 2004: Analysis of Multi-angle Imaging Spectroradiometer (MISR) aerosol optical depths over greater India during winter 2001–2004. *Geophys. Res. Lett.,* **31,** L23115, doi:10.1029/2004GL021273.

Jethva, H., S. K. Satheesh and J. Srinivasan, 2005: Seasonal variability of aerosols over Indo-Gangetic basin. *J. Geophys. Res.,* **110,** D21204, doi:10.1029/2005JD005938.

Kovalev, V. A., and W. E. Eichinger, 2004: *Elastic Lidar: Theory, Practice and Analysis Methods.* Wiley-Interscience, 615 pp.

Moorthy K. K., K. Niranjan, B. Narasimhamurthy, V. V. Agashe, and B. V. K. Murthy, 1999: Aerosol climatology over India, 1—ISRO GBP MWR network and database. ISRO GBP SR-03-99, Indian Space Research Organisation, Bangalore, India, 30 pp.

Ramanathan, V., and Coauthors, 2001: INDOEX aerosol forcing and climate impacts: An integrated assessment. *J. Geophys. Res.,* **106** (D22), 28 371–28 398.

Sagar, R., B. Kumar, U. C. Dumka, K. Krishna Moorthy, and P. Pant, 2004: Characteristics of aerosol spectral optical depths over Manora Peak: A high-altitude station in the central Himalayas. *J. Geophys. Res.,* **109,** D06207, doi:10.1029/2003JD003954.

Satheesh, S. K., and V. Ramanathan, 2000: Large difference in tropical aerosol forcing at the top of the atmosphere and Earth's surface. *Nature,* **405,** 60–63.

——, ——, B. N. Holben, K. K. Moorthy, N. G. Loeb, H. Maring, J. M. Prospero, and D. Savoie, 2002: Chemical, microphysical, and radiative effects of Indian Ocean aerosols. *J. Geophys. Res.,* **107,** 4725, doi:10.1029/2002JD002463.

Shaw, G. E., 1976: Error analysis of multi-wavelength sun photometry. *Pure Appl. Geophys.,* **114,** 1–14.

——, J. A. Regan, and B. M. Herman, 1973: Investigations of atmospheric extinctions using direct solar radiation measurements made with a multiple wavelength radiometer. *J. Appl. Meteor.,* **12,** 374–380.

Stull, R. B., 1989: *Boundary Layer Meteorology*. Kluwer, 620 pp.

Tripathi, S. N., S. Dey, V. Tare, and S. K. Satheesh, 2005: Enhanced layer of black carbon in a north Indian industrial city. *Geophys. Res. Lett.,* **32,** L12802, doi:10.1029/2005GL022564.